AIAA JOURNAL
Vol. 40, No. 6, June 2002

# Model for Active Control of Flow-Induced Noise Transmitted Through Double Partitions

Cedric Maury,* Paolo Gardonio,† and Stephen John Elliott‡
*University of Southampton, Highfield, Southampton, England SO17 1BJ, United Kingdom*

**The results are presented of a study concerned with the prediction of the airflow noise transmitted through an element of the fuselage structure: a double panel of finite extent that consists of a pair of thin elastic plates containing a light insulating material separated from the inner skin by an air gap. This configuration is representative of typical compound sidewalls in large commercial aircraft. A solution based on modal coupling is obtained and validated by comparisons with other solutions on various test cases. A physical interpretation is given for the calculated vibroacoustic response of a double partition system excited by a turbulent boundary layer, and the effect of an air gap between the insulation facing bag and the trim panel is analyzed. It is shown that the levels of the inwardly radiated sound power are mainly determined by the contribution of the first skin panel-controlled mode, and the added damping effect due to the insulating material has little effect below this resonance. To achieve sound reduction in the very low-frequency domain, the performance of various active control strategies are examined and compared. It is found that the most efficient strategy is the suppression of the low-order skin panel structural modes. However, we note that significant reductions in the sound power radiated can also be achieved by the active suppression of the low-order structural modes of the trim panel.**

## Nomenclature

| | | |
|---|---|---|
| $A_s$, $A_t$ | = | skin and trim panel surfaces |
| $\boldsymbol{a}$ | = | vector of cavity modes amplitudes |
| $\boldsymbol{C}$ | = | damping modal matrix |
| $C_e$ | = | cospectrum of the wall-pressure field |
| $c_a$ | = | sound speed of the equivalent fluid into the cavity |
| $c_e$ | = | external sound speed |
| $c_i$ | = | sound speed of the internal fluid |
| $c_j$ | = | equivalent fluid coefficients, $j = 1, \ldots, 8$ |
| $D_s$ | = | skin panel flexural rigidity |
| $d$ | = | cavity depth |
| $\boldsymbol{F}$ | = | vector of the cavity modes |
| $F_n$ | = | rigid wall cavity modes |
| $f_c$ | = | hydrodynamic coincidence frequency |
| $\boldsymbol{k}$ | = | wave number vector |
| $L_{s,nm}$, $L_{t,nm}$ | = | modal coupling coefficient between the $n$th cavity mode and the $m$th skin or trim panel mode |
| $l_x$, $l_y$ | = | respectively, spanwise and streamwise dimensions of the panels |
| $\boldsymbol{M}$ | = | mass modal matrix |
| $M_{i,m}$, $M_{a,n}$ | = | generalized masses associated to the $m$th panels mode and to the $n$th cavity mode |
| $N_a$ | = | number of cavity modes accounted for in the simulations |
| $N_s$, $N_t$ | = | number of skin and trim panels modes accounted for in the simulations |
| $P_i$ | = | amplitude of the incident pressure field |
| $p_a$ | = | cavity pressure field |
| $p_t$ | = | sound pressure radiated by the trim panel on its surface |
| $\boldsymbol{p}_t$ | = | vector of complex acoustic pressure at the trim panel surface |
| $\boldsymbol{Q}$ | = | eigenvector matrix of $\Re[\boldsymbol{Z}]$ |
| $\boldsymbol{Q}^e$ | = | vector of generalized forces |
| $Q^e_{s,m}$ | = | generalized external force associated to the $m$th skin panel mode |
| $\boldsymbol{q}_{\{s,t\}}$ | = | vector of complex structural modes amplitudes |
| $\Re[\boldsymbol{Z}]$ | = | modal radiation resistance matrix of the trim panel |
| $r_x$, $r_y$ | = | separation distances, respectively, in the spanwise and in the streamwise directions |
| $\boldsymbol{S}$ | = | stiffness modal matrix |
| $t$ | = | time |
| $U_c$ | = | convection velocity |
| $U_\infty$ | = | freestream velocity |
| $V$ | = | cavity volume |
| $W_i$ | = | incident sound power |
| $W_r$ | = | sound power radiated by the trim panel |
| $w_s$, $w_t$ | = | skin and trim panels deflections |
| $\boldsymbol{X}$ | = | vector of unknown modal amplitudes |
| $\boldsymbol{Z}$ | = | matrix of specific modal acoustic impedance |
| $\alpha_x$, $\alpha_y$ | = | empirical coefficients for the cospectrum of the excitation in the spanwise and streamwise directions, respectively |
| $\zeta_{i,m}$ | = | damping ratio of the $m$th structural mode |
| $\theta$ | = | incidence angle |
| $\Lambda$ | = | eigenvalue matrix of $\Re[\boldsymbol{Z}]$ |
| $\boldsymbol{\Xi}$ | = | spatial position vector |
| $\xi$ | = | nondimensional frequency parameter of the equivalent fluid model |
| $\rho_a$ | = | mass density of the equivalent fluid into the cavity |
| $\rho_e$ | = | external air density |
| $\rho_i$ | = | internal air density |
| $\rho_s$ | = | skin panel mass density |
| $\sigma$ | = | flow resistivity of the equivalent fluid |
| $\Phi_e$ | = | cross-spectral density function of the wall-pressure field |
| $\boldsymbol{\Phi}_{Q^e}$ | = | cross-spectral density matrix between the generalized forces of the excitation |
| $\Phi_{W_r}$ | = | spectrum of the acoustic power radiated by the trim panel |
| $\boldsymbol{\Phi}_{\alpha\beta}$ | = | cross-spectral density matrix between the random variables $\alpha$ and $\beta$ |

Presented as Paper 2001-2111 at the AIAA/CEAS 7th Aeroacoustics Conference, Maastricht, The Netherlands, 28–30 May 2001; received 31 May 2001; revision received 20 January 2002; accepted for publication 28 January 2002. 

*Research Fellow, Institute of Sound and Vibration Research.
†Lecturer, Institute of Sound and Vibration Research.
‡Professor of Adaptive Systems, Institute of Sound and Vibration Research.

$\Phi_0$ = point-power spectral density of the wall-pressure field
$\Psi_{\{s,t\}}$ = vectors of the skin and trim panels' structural mode
$\psi_{s,m}$, $\psi_{t,m}$ = skin and trim panels structural modes
$\omega$ = angular frequency
$\omega_{i,m}$, $\omega_{a,n}$ = eigenfrequencies associated to the $m$th panels mode and to the $n$th cavity mode
$\omega_{\mathrm{pcp},1}$ = first plate–cavity–plate resonance frequency

## I. Introduction

UNDER typical cruise conditions, the turbulent boundary-layer pressure fluctuations imparted on the exterior fuselage shell of a high-speed, jet-powered, well-streamlined aircraft constitute the most important source of cabin noise. The spectrum of the boundary-layer pressure is mostly significant at frequencies from below 100 to above 2000 Hz (Ref. 1). A representative model to describe noise transmission through aircraft sidewalls is to consider a fuselage double-panel system filled with an insulating bag. For airflow noise transmission problems, the outer panel is then excited by a turbulent boundary layer (TBL).

Sidewall treatments have been extensively studied[2,3] to find a way to reduce the airborne path for noise transmission through the fuselage structure. It has been shown that applying damping materials to the fuselage skin provides significant increases in sidewall transmission loss at high frequencies, especially where the sound transmission is governed by the resonant response of the skin structure. However, such treatments are inefficient below the fundamental frequency of the skin panel. Active noise control systems applied to aircraft sidewalls provide a potential solution to improve the reduction of noise due to TBL in this frequency range.

Although there are many experimental and theoretical studies on the sound transmission through fuselagelike structures and its control when driven at a single frequency, the number of models describing the response of aircraft sidewalls to random convected fields is more limited. One of the first analytical models was concerned with the boundary-layer noise transmitted through a flexible plate into a closed cavity.[4] A parametric analysis was carried out on the mutual interaction between the plate, the external flow, and the internal air cavity, with emphasis on the aerodynamic damping effect at high supersonic Mach numbers.

However, the problem of cavity-backed finite panels has been the subject of many more investigations in case of forced harmonic regimes, thus leading to a better understanding of structural–acoustic coupling between the panel and the cavity.[5,6] A general analytical formulation of this problem has been developed by Dowell et al., based on the expansion of the system response in terms of the eigenmodes of the uncoupled subsystems.[7] This computationally efficient method has been used by Sas et al. to understand the limitations in the performance of an active noise control system using small loudspeakers inserted into an air gap enclosed by two flexible panels.[8]

As an alternative, an analytical study based on modal acoustic transfer impedance and mobility matrices has been proposed by Pan and Bao to explain the mechanisms of attenuation associated with different control arrangements.[9] Experiments have confirmed that active control of sound transmission through double-panel partitions using either cavity control or radiating panel control is more effective than room control for global noise reduction.[10] Moreover, cavity control achieves better performances than panel control in the very low-frequency domain, whereas panel control becomes more efficient at higher frequencies. A recent paper on the active control of structure-borne and airborne sound transmission through an aircraft sidewall using a discretized version of the impedance and mobility matrix approach observed that, in the low-frequency domain, the airborne transmission path is dominant compared with the structure-borne transmission path and that control systems acting directly on the sound transmission–radiation mechanisms are, therefore, more effective.[11]

So far, these approaches do not account for a random excitation of the double-panel system. Thus, the main objective of this paper is to extend the previous analysis to the case of a turbulent boundary-layer excitation of a double-partition representative of an aircraft sidewall. From this model, a parametric analysis is conducted to understand the physics of the vibroacoustic phenomena involved but also to show the limited performances of passive treatments in the low-frequency domain. The effectiveness of several active control approaches for reducing sound transmission through aircraft sidewalls are then explored individually and compared. Among those strategies, the most feasible are based on active structural acoustic control (ASAC) of the radiating panel, and we examine the influence on the sound power radiated of either canceling the structural modes or the radiation modes of the trim panel.

## II. Theory

In this section, if we denote $f(\Xi; t)$, a function of the two-dimensional spatial vector $\Xi$ and time variable $t$, and $f(\boldsymbol{k}; \omega)$, its wave number frequency Fourier transform, which is a function of the wave number vector $\boldsymbol{k}$ and angular frequency variable $\omega$, then use is made of the following Fourier transform convention between these two quantities:

$$f(\boldsymbol{k}; \omega) = \int_{-\infty}^{+\infty} \mathrm{d}t \iint_{\infty} \mathrm{d}^2\Xi f(\Xi; t) \exp[-j(\omega t - k \cdot \Xi)] \quad (1)$$

### A. Double-Panel Model

In practice, lightweight fuselage shells are rather complicated structures because skin–stringer–frame constructions are commonly used for many commercial aircraft. However, measurements have shown that, depending on the frequency range of interest, different simplified models can be applied to describe accurately the vibrating response of the skin structure.[12] At high subsonic Mach numbers and for frequencies above 500 Hz, the vibrations between adjacent panels separated by frame lines are weakly correlated. Moreover, the stiffener motion becomes less important than the panel motion. Thus, the high-frequency panel model is appropriate to describe noise transmission through individual vibrating skin panels. Models valid at lower frequencies should consider an array of flexible panels reinforced by elastic stiffeners. For the purposes of this study, we will only concentrate on the high-frequency double-panel model. Because of the cabin pressurization, the influence of panel curvature on the interior sound level can be neglected.[13]

Figure 1 shows the double-panel model adopted to represent an aircraft fuselage section. The outer part of the double panel is assumed to be excited by a fully developed turbulent flow. The skin panel is modeled by a simply supported aluminium flat plate stressed by tension forces and set in an infinite rigid baffle. The dimensions of this panel are determined by the dimensions of neighboring circumferential doublers and longitudinal stringers, whereas the dimensions of the trim panel correspond to the dimensions of the region defined by adjacent frames and stringers, also referred to as a fuselage bay.[1] The trim panel is modeled by a simply supported flat composite plate set in an infinite rigid baffle. The cavity is assumed to contain an insulation bag filled with a dissipative material, which can be separated from the trim panel by an air gap. Because of the low density of the air and the high stiffness of the panels, the radiation loading has little effect on the panels' vibration.[14] Therefore, we can neglect the acoustical loading of both panels by the external fluid medium, which is small compared with their mutual coupling by the cavity, especially if it is a shallow cavity.[5] The geometrical and physical properties for the airflow, the two panels and the cavity are listed in Table 1 (see Ref. 1).

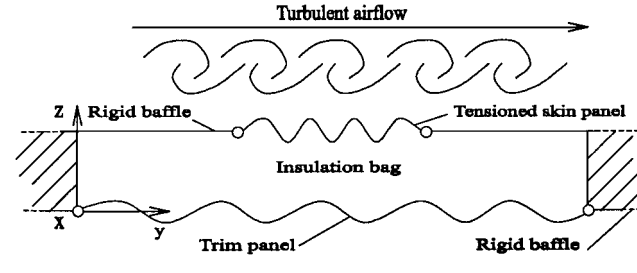


Fig. 1 Double-panel model.

**Table 1 Geometrical and physical parameters for a typical aircraft sidewall at the forward location**

| Parameter | Value |
|---|---|
| *Airflow* | |
| Freestream velocity | $U_\infty = 225$ m/s |
| RMS wall pressure | 72.6 N/m$^2$ |
| External air density | $\rho_e = 0.53$ kg/m$^3$ |
| External sound speed | $c_e = 310$ m/s |
| *Skin panel* | |
| Dimensions | $l_x = 0.20$ m, $l_y = 0.17$ m |
| Thickness | $h_s = 0.0015$ m |
| Mass density | $\rho_s = 2700$ kg/m$^3$ |
| Young's modulus | $7.1 \times 10^{10}$ Pa |
| Poisson ratio | 0.33 |
| Damping ratio | 0.01 |
| Streamwise tension | $29.3 \times 10^3$ N/m |
| Spanwise tension | $62.1 \times 10^3$ N/m |
| *Trim panel* | |
| Dimensions | $l_x = 0.20$ m, $l_y = 0.50$ m |
| Thickness | 0.004 m |
| Mass density | 255 kg/m$^3$ |
| Young's modulus | $1.5 \times 10^9$ Pa |
| Poisson ratio | 0.3 |
| Damping ratio | 0.05 |
| *Dissipative material (fiberglass)* | |
| Thickness | $d = 0.07$ m |
| Flow resistivity | $\sigma = 12000$ N m$^{-4}$s |
| Equivalent fluid constants | $c_1 = 0.070$, $c_2 = -0.632$ |
| | $c_3 = 0.107$, $c_4 = -0.632$ |
| | $c_5 = 0.160$, $c_6 = -0.618$ |
| | $c_7 = 0.109$, $c_8 = -0.618$ |

Note that, for the simulations presented in this paper, the outer part of the fuselage bay has been modeled by a single skin panel set in a rigid baffle. A more representative model would have been to consider three uncorrelated skin panels with the same total size as the trim panel. The only difference with this refined model concerns the coupling between the inner panel and the cavity in the very low-frequency domain, but it has been found that the results obtained by the simplified model are not qualitatively modified.

### B. Modal Formulation for the Vibroacoustic Problem

We use the modal formulation developed by Dowell et al.[7] because the success and the efficiency of the method has been largely demonstrated in the study of the response of a panel–cavity system.[7,8] In this method, the panels deflections $w_s$ and $w_t$ of the skin panel and the trim panel, respectively, are expanded as a finite series of $N_s$ and $N_t$ orthogonal functions, that is, the corresponding panels structural modes $\psi_{s,m}$ and $\psi_{t,m}$. The acoustic pressure field in the cavity $p_a$ is expanded as series of $N_a$ orthogonal functions, the rigid wall cavity modes $F_n$, so that

$$w_{\{s,t\}}(x, y; t) = \sum_{m=1}^{N_{\{s,t\}}} q_{\{s,t\},m}(t)\psi_{\{s,t\},m}(x, y) = \boldsymbol{\Psi}_{\{s,t\}}^T \boldsymbol{q}_{\{s,t\}} \quad (2)$$

$$p_a(x, y, z; t) = \sum_{n=0}^{N_a} a_n(t) F_n(x, y, z) = \boldsymbol{F}^T \boldsymbol{a} \quad (3)$$

where $\boldsymbol{\Psi}_{\{s,t\}}$ and $\boldsymbol{F}$ are, respectively, the $N_{\{s,t\}}$-length vectors of the panels structural mode shapes and the $N_a$-length vector of the rigid wall cavity mode shapes. Here, $\boldsymbol{q}_{\{s,t\}}$ and $\boldsymbol{a}$ both have second-order behavior.

When Eqs. (2) and (3) are substituted into the variational equations of motion for the panels and the acoustic cavity, a set of $(N_s + N_t + N_a + 1)$ coupled algebraic equations is obtained as follows[7,8]:

$$M_{i,m}\left[\ddot{q}_{i,m} + 2\zeta_{i,m}\omega_{i,m}\dot{q}_{i,m} + \omega_{i,m}^2 q_{i,m}\right] = \rho_a c_a^2 A_i \sum_{n=0}^{N_a} \dot{a}_n \left(\frac{L_{i,nm}}{M_{a,n}}\right) + Q_{s,m}^e, \qquad i = \{s, t\} \quad (4)$$

$$V\left[\ddot{a}_n + \left(\frac{c_a}{c_0}\right)^2 \omega_{a,n}^2 a_n\right] = -A_s \sum_{m=1}^{N_s} \dot{q}_{s,m} L_{s,nm} - A_t \sum_{m=1}^{N_t} \dot{q}_{t,m} L_{t,nm} \quad (5)$$

where $\{M_{i,m}, M_{a,n}\}$ are the generalized masses and $\{\omega_{i,m}, \omega_{a,n}\}$ the eigenfrequencies corresponding to the $m$th panels mode and to the $n$th cavity mode. $A_{\{s,t\}}$ and $V$ are the panels surfaces and the cavity volume, respectively. $\{Q_{s,m}^e\}$ are the generalized forces corresponding to the external pressures that act on the skin panel. Here $\rho_a$ and $c_a$ are used to model the acoustic properties of the dissipative material inside the cavity (see Sec. II.E). $L_{\{s,t\},nm}$ is the modal coupling coefficient between the $m$th panel mode and the $n$th cavity mode, which is given by

$$L_{\{s,t\},nm} = \frac{1}{A_{\{s,t\}}} \int_{A_{\{s,t\}}} F_n \psi_{\{s,t\},m}\, \mathrm{d}A \quad (6)$$

and represents a measure of the spatial matching between the $m$th panel mode and the $n$th cavity mode.

By the use of a matrix formulation, Eqs. (4) and (5) can be written as follows:

$$\boldsymbol{M}\ddot{\boldsymbol{X}} + \boldsymbol{C}\dot{\boldsymbol{X}} + \boldsymbol{S}\boldsymbol{X} = \boldsymbol{Q}^e \quad (7)$$

where $\boldsymbol{M}$ and $\boldsymbol{S}$ are the diagonal mass and stiffness matrices, $\boldsymbol{C}$ gathers the diagonal damping matrix and the sparse skew coupling matrix, $\boldsymbol{X}$ is the vector of the unknown complex modal amplitudes $\{\boldsymbol{q}_{\{s,t\}}; \boldsymbol{a}\}$ and $\boldsymbol{Q}^e = \{Q_{s,1}^e, \ldots, Q_{s,N_s}^e; 0, \ldots, 0; 0, \ldots, 0\}$.

We note that the resonance frequencies (or damped natural frequencies) and the corresponding resonance modes of the double-panel system are the nontrivial solutions, in the frequency domain, of the homogeneous system of equations associated to Eq. (7). When the cavity is filled with air, the resonance frequencies correspond to the eigenvalues of the coupled problem. They are calculated by a standard polynomial eigenvalue technique. When the cavity is filled with a porous material, its acoustic properties are frequency dependent, and the related eigenvalue problem is nonlinear. Because the eigenvalues depend analytically on the frequency, the argument theorem can then be used, in conjunction with Newton's method, first to isolate and second to approximate each resonance frequency in the complex frequency plane.[15]

In the case of a harmonic excitation of the double-panel system, the sound power radiated by the trim panel may be written as[16]

$$W_r = \tfrac{1}{2}\Re[\boldsymbol{p}_t \dot{\boldsymbol{q}}_t] \quad (8)$$

where $\boldsymbol{p}_t$ and $\dot{\boldsymbol{q}}_t$ are the $N_t$-length vectors of the modal amplitudes, respectively, associated to the complex acoustic pressure at the trim panel surface and to the velocity of the trim panel. These quantities are linked by the following relationship:

$$\boldsymbol{p}_t = \rho_i c_i \boldsymbol{Z}\dot{\boldsymbol{q}}_t \quad (9)$$

in which $c_i$ is internal sound speed. By the use of Eq. (9) for the vector of pressure modal amplitudes, the sound power radiated may be written as

$$W_r = \left(\rho_i c_i \omega^2 / 2\right) \boldsymbol{q}_t^H \Re[\boldsymbol{Z}] \boldsymbol{q}_t \quad (10)$$

where $\Re[\boldsymbol{Z}]$ is the modal radiation resistance matrix. Note that an efficient method due to Mangiarotty is used to compute each element of this matrix.[17] By the use of a set of linear transformations, the calculation of a quadruple integral for each element of the radiation matrix is then reduced to the evaluation of a double integral of a regular function over the transformed domain.

The case is first considered of excitation by an acoustic plane wave, in which case the sound transmission loss through the double-panel system is defined in terms of the ratio between the sound power incident on the skin panel and the sound power radiated by the trim panel $W_r$ as

$$\mathrm{TL(dB)} = 10\log(W_i / W_r) \quad (11)$$

where $W_i = |P_i|^2 l_x l_y \cos\theta / 2\rho_e c_e$.

### C. Double-Panel Response to a Random Excitation

Let us now consider the response of the double-panel system to a random stationary excitation. An example is the wall-pressure field due to a turbulent boundary layer, which is, strictly speaking, a weakly stationary process with respect to the time and space variables.[18] It is characterized by the following cross-spectral density (CSD) function:

$$\Phi_e(x, y, x', y'; \omega) = \Phi_0(\omega) C_e(x - x', y - y'; \omega) \tag{12}$$

where $\Phi_0(\omega)$ is the point-power spectral density of the wall-pressure field. We have chosen for $\Phi_0(\omega)$ a model arising from recent laboratory measurements.[19] The cospectrum $C_e$ is a measure of the spatial coherence of the excitation between two points. By the use of the Corcos model and according to the Fourier transform convention [Eq. (1)], it is given by[20]

$$C_e(r_x, r_y; \omega) = \exp(i\omega r_y / U_c) \exp(-\omega r_y / \alpha_y U_c) \times \exp(-\omega r_x / \alpha_x U_c) \tag{13}$$

where $r_x = x - x'$ and $r_y = y - y'$. $U_c \approx 0.7 U_\infty$ is the convection velocity and the empirical coefficients $\alpha_x$ and $\alpha_y$ are usually taken to be 1.2 and 8.

On introducing Eq. (12) into the input–output relationship between the CSD of the system response and the CSD of the excitation, we can establish that[21]

$$\boldsymbol{\Phi}\begin{Bmatrix} w_{s,t} \\ p_a \end{Bmatrix}\begin{Bmatrix} w_{s,t} \\ p_a \end{Bmatrix}(x, y, z, x', y', z'; \omega) = \begin{Bmatrix} \boldsymbol{\Psi}_{s,t}(x, y) \\ \boldsymbol{F}(x, y, z) \end{Bmatrix}^T \boldsymbol{\Phi}\begin{Bmatrix} q_{s,t} \\ a \end{Bmatrix}\begin{Bmatrix} q_{s,t} \\ a \end{Bmatrix}(\omega) \begin{Bmatrix} \boldsymbol{\Psi}_{s,t}(x', y') \\ \boldsymbol{F}(x', y', z') \end{Bmatrix} \tag{14}$$

The CSD between the complex modal amplitudes can be written as

$$\boldsymbol{\Phi}\begin{Bmatrix} q_{s,t} \\ a \end{Bmatrix}\begin{Bmatrix} q_{s,t} \\ a \end{Bmatrix}(\omega) = \boldsymbol{L}_\omega^{-1} \begin{bmatrix} \boldsymbol{\Phi}_{Q^e}(\omega) & \mathbf{0} & \mathbf{0} \\ \mathbf{0} & \mathbf{0} & \mathbf{0} \\ \mathbf{0} & \mathbf{0} & \mathbf{0} \end{bmatrix} \left(\boldsymbol{L}_\omega^{-1}\right)^H \tag{15}$$

where $\boldsymbol{L}_\omega = -\omega^2 \boldsymbol{M} + i\omega \boldsymbol{C} + \boldsymbol{S}$ and $\boldsymbol{\Phi}_{Q^e}$ is the $(N_s \times N_s)$ cross spectral density matrix between the generalized forces of the excitation. Exact analytical expressions can be derived for each element of $\boldsymbol{\Phi}_{Q^e}$, also called the joint acceptance functions.[22] However, at high subsonic Mach numbers, it can be shown that the skin panel structural modes are excited independently, that is, the cross terms in $\boldsymbol{\Phi}_{Q^e}$ are small compared to the diagonal terms and $\boldsymbol{\Phi}_{Q^e}$ is well approximated by its main diagonal.[23]

The spectrum of the acoustic power radiated by the trim panel is given by

$$\Phi_{W_r}(\omega) = \frac{1}{2} \Re \left[ \int_{A_t} \Phi_{p_t \dot{w}_t}(x, y; \omega)\, dx\, dy \right] \tag{16}$$

On using Eq. (14) and the integral representation of $p_t$ in terms of $\dot{w}_t$, we find

$$\Phi_{W_r}(\omega) = \left(\rho_i c_i \omega^2 / 2\right) \operatorname{tr}[\boldsymbol{\Phi}_{q_t q_t} \Re[\boldsymbol{Z}]] \tag{17}$$

where $\Re[\boldsymbol{Z}]$ is the modal radiation resistance matrix used in Eq. (10).

### D. Radiation Modes

The modal radiation resistance matrix $\Re[\boldsymbol{Z}]$ is real, symmetric, and positive definite. An eigenvalue/eigenvector decomposition of $\Re[\boldsymbol{Z}]$ can be written as

$$\Re[\boldsymbol{Z}] = \boldsymbol{Q} \Lambda \boldsymbol{Q}^H \tag{18}$$

where $\boldsymbol{Q}$ is the unitary matrix of eigenvectors and $\Lambda$ is the diagonal matrix of eigenvalues, which are all real and positive. When Eq. (18) is used, the sound power radiated by the trim panel under a harmonic excitation, Eq. (10), now becomes

$$W_r = \frac{\rho_i c_i \omega^2}{2} \boldsymbol{b}_t^H \Lambda\, \boldsymbol{b}_t = \frac{\rho_i c_i \omega^2}{2} \sum_{m=1}^{P_t} \Lambda_m |b_{t,m}|^2 \tag{19}$$

where $\boldsymbol{b}_t = \boldsymbol{Q}^H \boldsymbol{q}_t$ is the vector of transformed modes amplitudes. From Eq. (19), it is clear that the transformed modes or radiation modes radiate sound independently of each other.[16] Because the radiation resistance matrix $\Re[\boldsymbol{Z}]$ is frequency dependent, the shape of the radiation modes also depend on frequency, unlike the classical modes. In particular, it can be shown that the first radiation mode is well approximated at low frequencies by the net volume velocity of the panel.[16] The contribution of this mode to the acoustic power is most important at low frequencies, and so significant reductions in the sound power radiated can be achieved by controlling this single mode. For harmonic excitation, it can be significantly more efficient to control actively radiation mode amplitudes than structural mode amplitudes, although this advantage is not so pronounced when a single panel is excited by a TBL.[24] In Sec. VI, both control strategies will be considered for the control of the TBL-excited double-panel system defined earlier.

### E. Equivalent Fluid Model of the Insulating Material

Insulation bags containing layers of porous materials are inserted between the skin and trim panels in each frame bay to limit heat transfer and acoustic transmission as indicated in Fig. 1. Much research has been devoted to wave propagation through such materials, and a rigorous description should consider poroelastic modeling, that is, both airborne and structure-borne transmission through the medium.[25] However, as shown by Beranek, longitudinal elastic waves are generally much more attenuated than the acoustic compression wave that propagates through insulating materials with a relatively low frame stiffness such as unreinforced fiberglass.[26] The porous material used in insulation bags is often of this form, and so an equivalent fluid model can be used to describe the vibration transmission between the panels.

The equivalent fluid parameters are a complex effective density $\rho_a$ and sound speed $c_a$ that are both frequency dependent. They are given, in terms of the empirical constants listed in Table 1, by[27]

$$\rho_a(f) = \rho_i c_i \left[1 + c_1 \xi^{c_2} - i c_3 \xi^{c_4}\right] / c_a(f)$$
$$c_a(f) = c_i \Big/ \left[1 + c_7 \xi^{c_8} - i c_5 \xi^{c_6}\right] \tag{20}$$

where the nondimensional frequency is equal to $\xi = f\rho_i / \sigma$ and $\sigma$ is the flow resistivity.

## III. Comparison with Different Methods in Harmonic Regime

To validate the vibroacoustic model for the double-panel system, comparisons have been made on a test case between our predictions and the results from two alternative analysis methods. We have considered a double-plate system containing an air cavity enclosed between two simply supported identical panels. The outer panel is excited by a normal incident plane wave of unit pressure amplitude (1 N/m$^2$). Each panel is aluminum made and is assumed to have dimensions $350 \times 220 \times 1$ mm$^3$ thick, with a constant modal damping ratio of 1%. The cavity depth is 76.2 mm. The modal damping ratio of the air cavity is 1%. These parameters are those used in a recent study on the finite element/boundary element computation of the sound transmitted through a double-partition system.[28]

The sound transmission loss (decibels) using our model is plotted as the solid line in Fig. 2. The dashed line corresponds to numerical predictions issued from a discretized impedance and mobility matrix approach.[11] The agreement is excellent, and these results also compare very well with those published by Panneton et al.[28]

Figure 2 shows very poor transmission loss for these panels at low frequencies. An improvement in the transmission loss is observed at higher frequencies. The first and third dips in Fig. 2 are due to odd–odd resonances of the panels, the fourth dip to a cavity resonance, and the second dip to a plate–cavity–plate resonance. At this frequency (157 Hz), a decrease of almost 30 dB is observed in the transmission loss. In particular, it corresponds to the first bending mode of the panels when they vibrate out of phase, that is, the (1, 1) mode, whereas, at the first dip at about 70 Hz, the panels vibrate in phase on the same first mode. In the latter case, the added mass effect of the air cavity results in a very small decrease of the first panel

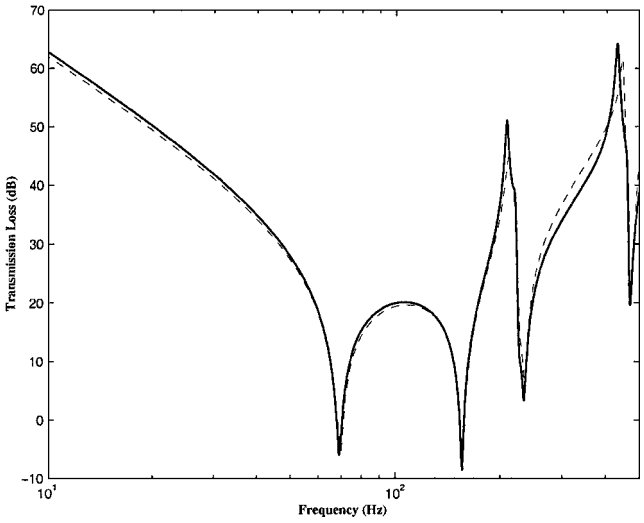


**Fig. 2 Normal incidence sound transmission loss through a double panel; comparison between ——, a modal approach; and - - -, a mobility approach.**

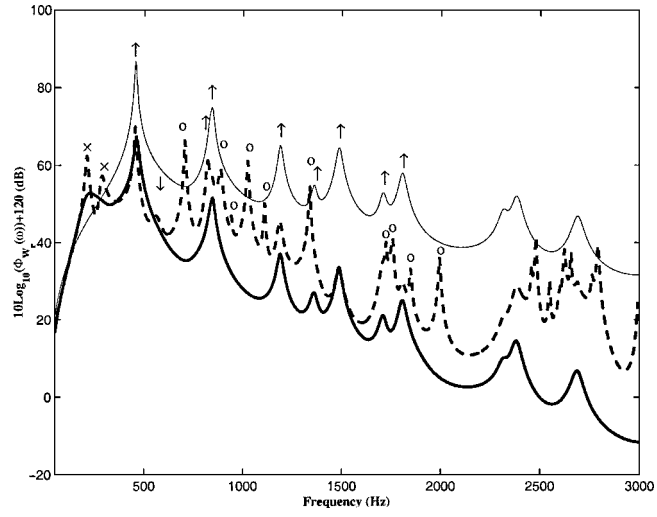


**Fig. 3 Sound power radiated inward by an aircraft sidewall excited by a TBL: ⊙⊙⊙, skin panel alone; - - -, double panel with air cavity; and ——, double panel with fiberglass cavity. The crosses denote a plate–cavity–plate resonance, the up arrows, a skin panel-controlled resonance; the down arrows, a trim panel-controlled resonance; and the ○, a cavity-controlled resonance.**

resonant frequency. In the first case, there is a significant increase in the first panel resonant frequency due to an important coupling with the (0, 0, 0) uniform pressure cavity mode that gives rise to equivalent stiffness. From Eqs. (2–3), it can be shown that the first plate–cavity–plate resonant frequency can be well approximated by

$$\omega^2_{\text{pcp},1} \approx \omega^2_{s,1} + \frac{2\rho_a c_a^2 A_s^2}{V M_{s,1}} L^2_{s,01} \tag{21}$$

This formula predicts, in our case, the first plate–cavity–plate resonance at 163 Hz, that is, with an error less than 3.7%. Other plate–cavity–plate resonances occur but to a lesser extent because it is the first panel mode that is mostly influenced by the (0, 0, 0) cavity mode.

It can be concluded that the vibroacoustic model we have chosen provides satisfactory results in the harmonic regime. We now analyze the predictions obtained for a TBL excitation.

## IV. Numerical Results with a TBL Excitation

Results will now be discussed for two design configurations: the case where the panels are bonded directly to the surfaces of the fiberglass layer and the case where the skin panel is bonded to the outer face of the insulating layer, whereas the trim panel is separated from the inner face of the fiberglass by an air gap.

### A. Equivalent Fluid in Entire Cavity

The numerical results presented here have been calculated for the physical and geometrical parameters listed in Table 1. To ensure convergence of the results up to 3 kHz, we have considered up to ($N_{s,x} = 3$, $N_{s,y} = 9$) structural modes for the skin panel, up to ($N_{t,x} = 4$, $N_{t,y} = 11$) structural modes for the trim panel, and up to ($N_{a,x} = 3$, $N_{a,y} = 3$, $N_{a,z} = 2$) cavity modes.

Figure 3 shows a comparison between the sound power radiated inward by a single skin panel, by the double-panel system with air between the panels, and by the double-panel system with the equivalent fluid between the panels, all excited by the TBL. We note that the vibroacoustic response of the skin panel alone is significantly modified when backed by an air cavity with one flexible wall (dashed line): the resonant behavior of the cavity is easily seen, and plate–cavity–plate resonances are observed below 500 Hz, where the (0, 0, 0) cavity mode induces significant changes in the trim panel first resonant frequencies. Above 500 Hz, the plate–cavity–plate resonances can be interpreted as perturbed structural or cavity resonances, that is, panel-controlled resonances or cavity-controlled resonances. In this frequency range, we also observe that the trim panel-controlled modes are so damped that they do not contribute significantly to the response of the panel–air–panel system. Therefore, we are left with skin panel-controlled modes and cavity-controlled modes.

When fiberglass is inserted within the cavity, the cavity-controlled modes are so damped that the resonant behavior of the cavity is not seen. In this configuration, the vibroacoustic response of the panel–fiberglass–panel system is mainly governed by skin panel controlled modes. Above the first skin panel resonant frequency, the finite size of the insulating materials and trim panel can, thus, be neglected in the prediction of boundary-layer noise in the aircraft. A much simpler but still representative model for boundary-layer noise transmission through aircraft sidewalls above about 500 Hz would, therefore, be a simply supported skin panel, set in an infinite rigid baffle and in contact with an infinite layer of dissipative material backed by an infinite trim plate.[29]

Another important feature seen in Fig. 3 is the added damping effect induced by the absorbent material on both the plate–air–plate resonances and the structural resonances. It leads to an overall sound power reduction that increases toward high frequencies compared with the single panel case. However, only a 4-dB reduction is observed for the total sound power radiated up to 3 kHz by the panel–fiberglass–panel system compared with the panel–air–panel system. Such a result is not surprising because it is the first skin panel-controlled resonance that determines the overall level of sound power radiated, and the contribution of this resonance to the sound power levels is weakly modified by the insertion of the fiberglass treatment.

Figure 3 also shows that, below 2 kHz, the contribution of some other skin panel-controlled modes to the sound power inwardly radiated is weakly affected by the insertion of insulating material. As a whole, these are the (1, 1) mode occurring at 453 Hz, the (1, 2) mode at 839 Hz, and the (1, 3) mode at 1484 Hz. To explain the significant contribution of these modes to the system response, the modal joint acceptances of skin panel modes have been plotted in Fig. 4.

The modal joint acceptances represent a measure of the spatial match between the convective scale of the turbulent excitation, where the main fluctuating energy lies, and the scale of each panel mode. For each mode, the main maximum occurs at the hydrodynamic coincidence frequency determined by $f_c^{m_{s,y}} = m_{s,y} U_c / 2 l_y$, where $m_{s,y}$ is the streamwise modal order. We observe that, when the (1, 1), (1, 2), and (1, 3) modes are resonant, they are also highly correlated with the wall-pressure fluctuations, whereas, for instance, the (1, 4) mode and (2, 4) mode, at their excitation frequencies of 2379 and 2685 Hz, respectively, are no longer coincident with the forcing field. A guideline to determine the frequency range above which resonant modes cannot be coincident is determined

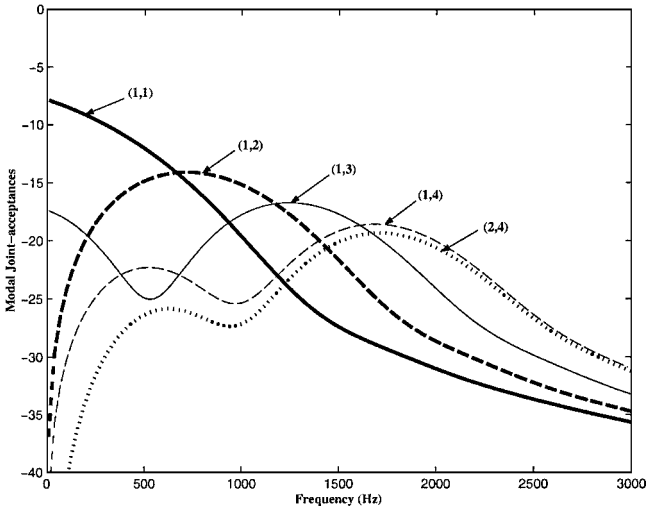


**Fig. 4 Modal joint acceptances for the simply supported skin panel subjected to a turbulent boundary layer: ——, (1, 1) mode; − − −, (1, 2) mode; ⊙⊙⊙, (1, 3) mode; ⊙⊙⊙, (1, 4) mode; and · · · ·, (2, 4) mode.**

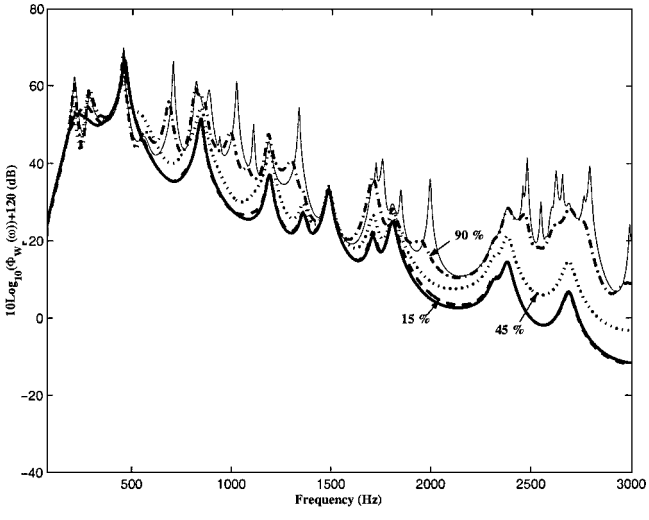


**Fig. 5 Influence of the air gap thickness on the sound power inwardly radiated by an aircraft sidewall under a TBL excitation: ——, bonded–bonded case; − − −, bonded–unbonded case with an air gap of 15% of the cavity depth; · · · ·, 45% of the cavity depth; ·−·−, 90% of the cavity depth; and ——, air cavity case.**

by equating the panel flexural wave speed and the flow convection velocity.[22] It is given by $2\pi f_c = U_c^2\sqrt{(\rho_s h_s/D_s)}$, where $\rho_s h_s$ is the mass density per unit area of the skin panel. It corresponds to an upper frequency of 2450 Hz for the untensioned skin panel. Because of pressurization effects, the skin panel resonant frequencies are shifted up, and the hydrodynamic coincidence frequency range is consequently reduced. According to our simulations, no coincident and resonant modes are observed above 2 kHz. This is in accordance with the fact that, as observed in Fig. 3, above 2 kHz, no skin panel-controlled mode is excited with enough efficiency to overcome the added damping effect due to the cavity treatment.

### B. Equivalent Fluid Only in a Proportion of Cavity

We now examine the influence of an air gap separating the insulation bag facing from the trim panel. In Fig. 5, the spectrum of the sound power radiated has been calculated for various air gap depths. As expected, when the air gap thickness increases, the spectrum in the bonded–bonded case gradually tends toward the spectrum in the air cavity case shown in Fig. 3. We also observe that the introduction of a fiberglass layer with a thickness equal to only 10% of the cavity depth is sufficient to suppress the resonant behavior of the cavity.

The most important feature of Fig. 5, however, is that, because we can neglect the frame waves transmission within fiberglass material, there is very little difference in terms of the sound power radiated between the bonded–bonded case and the bonded–unbonded case with a thin air gap (15% of the cavity depth). Such a conclusion has also been observed by Panneton and Atalla.[28]

From Fig. 5, it is evident that the fiberglass treatment starts to be efficient only above the first skin panel-controlled resonance, that is, 500 Hz. Below this frequency, the performance for the treated case and the untreated case are similar. It is, therefore, of interest to investigate the performance of active control strategies in this frequency range. Note that, although the model described in Sec. II.A is, strictly speaking, valid only above 500 Hz, recent calculations have shown that the results concerning the performance of active control strategies below 500 Hz are not dramatically modified if elastic reinforcements between each skin panel are included.

## V. Limitations of Active Control Performances for a TBL Excitation

We now examine the limitation performances of ASAC and cavity control to compensate, in the low-frequency domain, for the poor noise reduction obtained by inserting insulating materials into the double-panel cavity. In practice, two ASAC strategies could be considered to reduce the sound power radiated by the trim panel.[30,31] We can either control the first structural modes or the first radiation modes of this panel. In Sec. V.A, we compare active systems that control the structural modes of either the trim panel or the skin panel with systems that control the modes of the cavity. In Sec. V.B, we consider the control of the trim panel radiation modes, which are frequency dependent.

In practice, the design of a sensor/controller/actuator arrangement that could excite/detect only one of these radiation modes over any frequency bandwidth is not physically possible. However, in a first step, suppressing the contribution of these modes from the modal summations used to calculate the double-panel response provides an upper limit in the performance of a collocated actuator/sensor pair. Indeed, this type of idealized feedback control system has been shown to achieve good performances to an arbitrary excitation while ensuring unconditional stability because the feedback gain can be made arbitrarily large.[24]

### A. Panels' Structural Modes Control and Cavity Control

To define a suitable control strategy, we first examine the reductions obtained in the inwardly radiated sound power [Eq. (17)] by canceling the participation of the first modes of different subsystems: the trim panel structural modes (Fig. 6), the skin panel

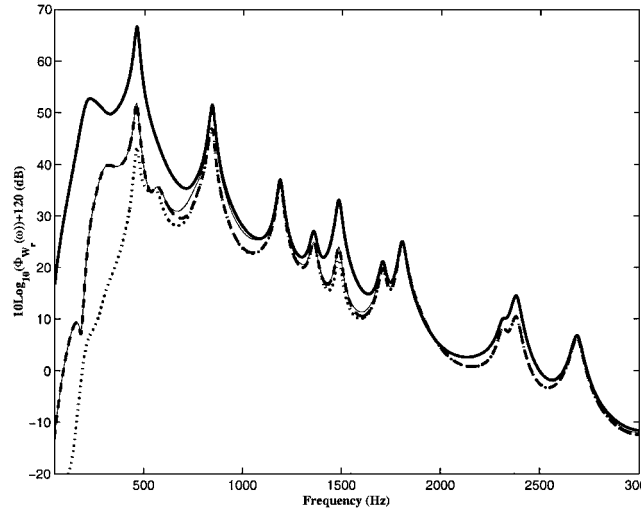


**Fig. 6 Sound power inwardly radiated by the double-panel system when controlling the structural modes of the trim panel: ——, before control; ⊙⊙⊙, after cancellation of the first structural mode of the trim panel; − − −, after cancellation of its two first structural modes; and · · · ·, after cancellation of its three first structural modes.**

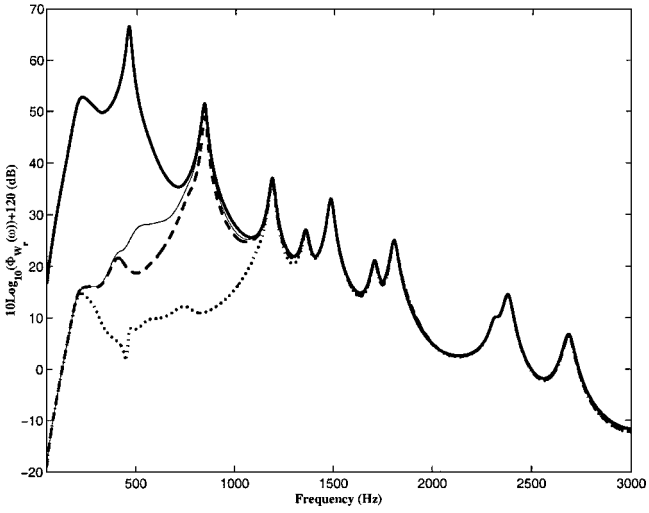


**Fig. 7 Sound power inwardly radiated by the double-panel system when controlling the structural modes of the skin panel: ——, before control; ⊙⊙⊙, after cancellation of the first structural mode of the skin panel; – – –, after cancellation of its two first structural modes; and · · · ·, after cancellation of its three first structural modes.**

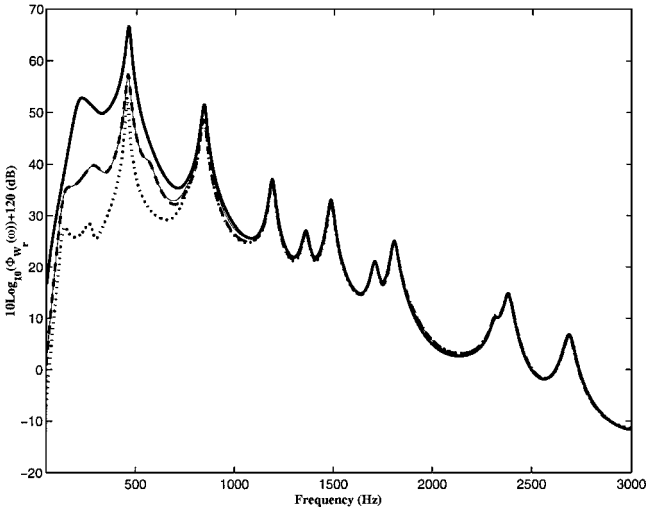


**Fig. 8 Sound power inwardly radiated by the double-panel system when controlling the cavity modes: ——, before control; faint ——, after cancellation of the first cavity mode; – – –, after cancellation of the two first cavity modes; and · · · ·, after cancellation of the three first cavity modes.**

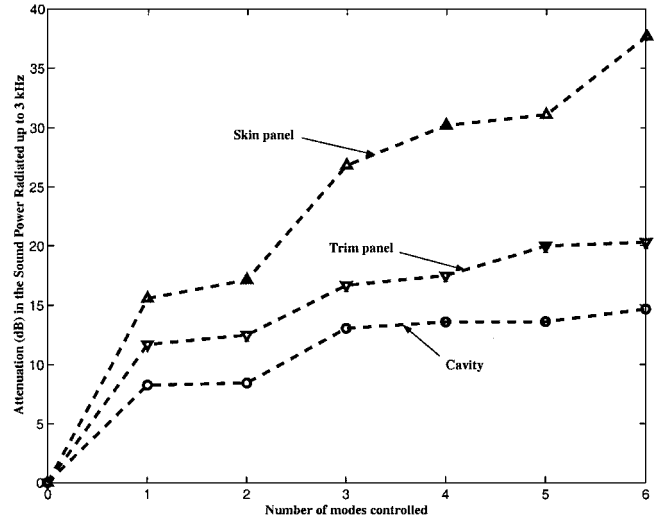


**Fig. 9 Attenuation in the total sound power radiated by the double-panel system up to 3 kHz: ▲, after cancellation of the first structural modes of the skin panel; ▼, after cancellation of the first structural modes of the trim panel; and ○, after cancellation of the first cavity modes.**

structural modes (Fig. 7) and the cavity modes (Fig. 8). The performances are summarized in Fig. 9.

An important feature for the double-panel system is that the structural modes of both panels are mutually coupled through the shallow cavity, especially in the very low-frequency domain. From Fig. 6, it can be seen that this coupling has a beneficial effect on modal suppression. Indeed, canceling the contribution of the first trim panel structural mode also reduces the contribution of all of the skin panel modes that couple well with this trim panel mode, especially the first structural mode of the skin panel, which mostly contributes to the total sound power inwardly radiated.

However, as explained in Sec. IV, most of the resonances that contribute to the double-panel response are controlled by the skin panel resonances: they correspond to the skin panel structural modes that are both coincident and resonant. From Fig. 7, we observe, as expected, that canceling the contribution of these modes leads to an important reduction for the total sound power radiated (up to 16-dB reduction after suppression of the first structural mode). As seen from Fig. 9, when the higher-order structural modes are canceled, sound power reductions are achieved more efficiently when suppressing the contribution of the skin panel modes compared with the trim panel modes.

From Fig. 8, we note that the cancellation of the first cavity modes does not involve a significant reduction in the sound power radiated up to 3 kHz and, as observed by Bao and Pan for tonal excitation, is only efficient in the very low-frequency domain.[10]

A comparison of the performances associated with each strategy can be interpreted in terms of the modal overlap of each subsystem (i.e., the average number of modes that falls within the bandwidth of any one mode at a given frequency) and the nature of the panel–cavity coupling. We note that the modal overlap of both panels increases linearly with frequency, the trim panel modal overlap being greater than the tensioned skin panel modal overlap. The modal overlap in the cavity is a quadratic function of frequency in this region. The nature of the panel–cavity coupling is determined by the average number of panels modes in the region of the natural frequency of a cavity mode. The three first cavity modes are below 700 Hz, and the skin panel modal overlap is very small in this frequency region. As observed in Figs. 7 and 9, because very few panel modes couple with the cavity modes in this frequency range, we can achieve a good sound reduction with only one control source. Because the trim panel modal overlap is higher in this frequency range, more trim panel modes couple with the cavity and the performances achieved with a limited number of control sources are reduced. Because the cavity modal overlap increases quadratically with frequency, it is expected that the control of the acoustic modes with a limited number of independent sources is only efficient in the very low-frequency domain, as confirmed by the results shown in Figs. 8 and 9.

In summary, it can be seen that the strategy based on the suppression of the skin panel structural modes is the most efficient in terms of attenuation of the total inwardly radiated sound power.

### B. Trim Panel Control: Structural Modes vs Radiation Modes Cancellation

Figure 10 summarizes the attenuation achieved for the total sound power radiated up to 3 kHz by suppressing a limited number of higher-order structural or radiation modes of the trim panel. We observe that approximately the same level of attenuation (about 12 dB) can be achieved by canceling the first structural mode or radiation mode of the trim panel. When higher-order modes are suppressed, the sound power reduction is slightly more significant when canceling the contribution of the structural modes compared with the radiation modes. From Fig. 6, we observe that the cancellation of the first structural modes provides sound reduction not only in the low-frequency domain where these modes are resonant but also at

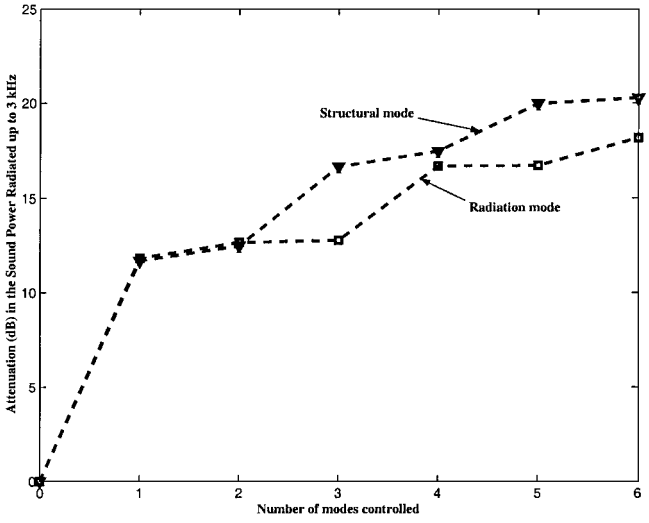


**Fig. 10 Attenuation in the total sound power radiated by the double-panel system up to 3 kHz: □, after cancellation of the first radiation modes of the trim panel; and ▼, after cancellation of its first structural modes.**

higher frequencies where other structural modes of the trim panel, which are mutually coupled with them through the fluid cavity, become resonant. However, note that, when suppressing the very first structural modes of the trim panel, the reduction induced by the contribution of these coupled modes is far less important than the reduction induced by the participation of the first structural modes. On the other hand, we have observed that the cancellation of higher-order radiation modes does not involve sound power reduction in the very low-frequency domain but only at higher frequencies for those sets of structural modes that have a multipolelike contribution to the sound pressure radiated. Consequently, suppressing higher-order radiation modes on the trim panel is less efficient than suppressing higher-order structural modes, as observed for the single TBL-excited panel.[24] Thus, we have shown that the maximum reductions predicted in the total sound power, radiated up to 1 kHz by a single skin panel excited by a TBL after canceling the contribution of the first radiation mode, are of the same order as the attenuations observed in an experimental study on active control of TBL-induced sound radiation from panels.[30,31]

## VI. Conclusions

In this paper, we have presented a simplified model to describe the boundary-layer noise transmitted through aircraft sidewalls. This model has been successfully compared with other methods when subject to harmonic excitation. The results predicted with a TBL excitation of the panel–fiberglass–panel system confirm that there is very little difference in terms of the sound power radiated between the bonded–bonded case and the bonded–unbonded case with a small air gap. The fiberglass treatment starts to be efficient only above the first skin panel-controlled resonance, that is, above about 500 Hz in our case. In this frequency range, the vibroacoustic response of the system is essentially governed by the modes of the skin panel. This suggests the use of a much simpler but still representative system for modeling aircraft sidewalls that can be obtained by neglecting the finite size effect of the cavity and trim panel.

The added damping effect induced by the insulating material is not pronounced below 500 Hz. To overcome this problem, the performance of various active control strategies have been investigated.

It has been shown that the most efficient strategy for this TBL-excited double-panel system is the suppression of the skin panel's structural modes. This strategy could provide attenuation up to 16 dB with a single control channel. However, this strategy may be difficult to implement in practice because of the need to bond actuators and sensors on the skin panels, which are repeatedly tensioned and untensioned due to pressurization. It may be more feasible to control the vibration of the trim panel or the pressure in the cavity, and these simulations suggest that the inwardly radiated sound power can still be reduced by about 12 dB, if only the first structural mode of the trim panel is actively controlled, or by about 8 dB, if the first acoustic mode of the cavity is actively controlled. As previously observed in a study of TBL transmission through single panels, however, there appears to be no advantage in controlling the trim panel's radiation modes rather than its structural modes when it is excited by a TBL via the skin panel and cavity.[24]

Because idealized and collocated sensor/actuator arrangements have been assumed in this paper, the performance has not been degraded by any spillover effects. In practice, the predicted results obtained when using feedback control techniques will always be degraded by issues associated with the selection of discrete actuators and sensors, model fidelity, and controller design. However, the object here was to derive the performance limitations due to the physical properties of the double-panel system excited by a TBL, rather than a particular actuator–sensor arrangement, and so the results provide an upper bound on the possible reductions achieved when using modal cancellation techniques.

The maximum gains predicted in the sound power radiated by double-panel partitions excited by a TBL have not yet been compared with any known previous experience. However, we have shown that the maximum reductions predicted in the total sound power, radiated up to 1 kHz by a single skin panel excited by a TBL after canceling the contribution of the first radiation mode, are of the same order as the attenuations observed in an experimental study on active control of TBL-induced sound radiation from panels.[30,31]

## References

[1]Wilby, J. F., and Gloyna, F. L., "Vibration Measurements of an Airplane Fuselage Structure, Part I: Turbulent Boundary Layer Excitation," *Journal of Sound and Vibration*, Vol. 23, No. 4, 1972, pp. 443–466.

[2]Vaicatis, R., "Noise Transmission into a Light Aircraft," *Journal of Aircraft*, Vol. 17, No. 2, 1980, pp. 81–86.

[3]Heitman, K. E., and Mixson, J. S., "Laboratory Study of Cabin Acoustic Treatments Installed in an Aircraft Fuselage," *Journal of Aircraft*, Vol. 23, No. 1, 1986, pp. 32–38.

[4]Dowell, E. H., "Transmission of Noise from a Turbulent Boundary Layer through a Flexible Plate into a Closed Cavity," *Journal of the Acoustical Society of America*, Vol. 46, No. 1, 1969, pp. 238–252.

[5]Pretlove, A. J., "Forced Vibrations of a Rectangular Plate Backed by a Cavity," *Journal of Sound and Vibration*, Vol. 3, No. 3, 1966, pp. 252–261.

[6]Guy, W. R., and Bhattacharya, M. C., "The Transmission of Sound through a Cavity-Backed Finite Plate," *Journal of Sound and Vibration*, Vol. 27, No. 2, 1973, pp. 207–223.

[7]Dowell, E. H., Gorman, G. F., and Smith, D. A., "Acoustoelasticity: General Theory, Acoustic Natural Modes and Forced Response to Sinusoidal Excitation, Including Comparisons with Experiments," *Journal of Sound and Vibration*, Vol. 52, No. 4, 1977, pp. 519–542.

[8]Sas, P., Bao, C., Augusztinovicz, F., and Desmet, W., "Active Control of Sound Transmission Through a Double Panel Partition," *Journal of Sound and Vibration*, Vol. 180, No. 4, 1995, pp. 609–625.

[9]Pan, J., and Bao, C., "Analytical Study of Different Approaches for Active Control of Sound Transmission Through Double Walls," *Journal of the Acoustical Society of America*, Vol. 103, No. 4, 1998, pp. 1916–1922.

[10]Bao, C., and Pan, J., "Experimental Study of Different Approaches for Active Control of Sound Transmission Through Double Walls," *Journal of the Acoustical Society of America*, Vol. 102, No. 3, 1997, pp. 1664–1670.

[11]Gardonio, P., and Elliott, S. J., "Active Control of Structure-Borne and Airborne Sound Transmission Through Double Panel," *Journal of Aircraft*, Vol. 36, No. 2, 1999, pp. 1023–1032.

[12]Mixson, J. S., and Wilby, J. F., "Aeroacoustics of Flight Vehicles: Theory and Practice," NASA TR 90-3052, 1991, pp. 271–355.

[13]Graham, W. R., "The Influence of Curvature on the Sound Radiated by Vibrating Panels," *Journal of the Acoustical Society of America*, Vol. 98, No. 3, 1995, pp. 1581–1595.

[14]14. Pan, J., and Bies, D. A., "The Effect of Fluid–Structural Coupling on Sound Waves in an Enclosure—Theoretical Part," *Journal of the Acoustical Society of America*, Vol. 87, No. 2, 1990, pp. 691–707.

[15]Maury, C., Filippi, P. J. T., and Habault, D., "Boundary Integral Equations Method for the Analysis of Acoustic Scattering from Line-2 Elastic Targets," *Flow, Turbulence and Combustion*, Vol. 61, No. 1, 1999, pp. 101–131.

[16]Elliott, S. J., and Johnson, M. E., "Radiation Modes and the Active Control of Sound Power," *Journal of the Acoustical Society of America*, Vol. 94, No. 4, 1993, pp. 2194–2204.

[17]Mangiarotty, R. A., "Acoustic Radiation Damping of Vibrating Structures," *Journal of the Acoustical Society of America*, Vol. 35, No. 3, 1963, pp. 369–377.

[18]Smol'yakov, A. V., and Tkatchenko, V. M., *The Measurement of Turbulent Fluctuations: an Introduction to Hot-Wire Anemometry and Related Transducers*, 1st ed., Springer-Verlag, Berlin, 1983, pp. 1–45.

[19]Durant, Ch., "Etude Experimentale de l'Excitation et de la Reponse Vibroacoustique d'une Conduite Sollicitee par un Ecoulement Interne," Ph.D. Dissertation 99-36, Ecole Centrale de Lyon, Laboratoire de Mecanique des Fluides et d'Acoustique, Unite Mixte de Recherche 5509, Lyon, France, July 1999.

[20]Corcos, G. M., "The Resolution of Turbulent Pressure at the Wall of a Boundary Layer," *Journal of Sound and Vibration*, Vol. 6, No. 1, 1967, pp. 59–70.

[21]Maury, C., Gardonio, P., and Elliott, S. J., "Model for the Control of the Sound Radiated by an Aircraft Panel Excited by a Turbulent Boundary Layer," Inst. of Sound and Vibration Research, TR-287, Univ. of Southampton, Southampton, England, U.K., June 2000.

[22]Robert, G., "Modelisation et Simulation du Champ Excitateur Induit sur une Structure par une Couche Limite Turbulente," Ph.D. Dissertation 84-02, Ecole Centrale de Lyon, Laboratoire de Mecanique des Fluides et d'Acoustique, Unite Mixte de Recherche 5509, Lyon, France, Jan. 1984.

[23]Davies, H. G., "Sound from Turbulent Boundary Layer Excited Panels," *Journal of the Acoustical Society of America*, Vol. 55, No. 2, 1971, pp. 213–219.

[24]Maury, C., Gardonio, P., and Elliott, S. J., "Active Control of the Flow-Induced Noise Transmitted Through a Panel," *AIAA Journal*, Vol. 39, No. 10, 2001, pp. 1860–1867.

[25]Biot, M. A., "The Theory of Propagation of Elastic Waves in a Fluid-Saturated Porous Solid," *Journal of the Acoustical Society of America*, Vol. 28, No. 1, 1956, pp. 168–191.

[26]Beranek, L. L., "Acoustical Properties of Homogeneous, Isotropic Rigid Tiles and Flexible Blankets," *Journal of the Acoustical Society of America*, Vol. 19, No. 4, 1947, pp. 556–568.

[27]Bies, D. A., "Acoustical Properties of Porous Materials," *Noise and Vibration Control*, 1st ed., edited by L. L. Beranek, McGraw–Hill, New York, 1971, pp. 245–269.

[28]Panneton, R., and Atalla, N., "Numerical Prediction of Sound Transmission Through Finite Multilayer Systems with Poroelastic Materials," *Journal of the Acoustical Society of America*, Vol. 100, No. 1, 1996, pp. 346–354.

[29]Graham, W. R., "Boundary Layer Induced Noise in Aircraft, Part II: The Trimmed Flat Plate Model," *Journal of Sound and Vibration*, Vol. 192, No. 1, 1996, pp. 121–138.

[30]Gibbs, G. P., Cabell, R. H., and Juang, J., "Controller Complexity for Active Control of Turbulent Boundary Layer Induced Sound Radiation from Panels," AIAA Paper 2000-2043, June 2000.

[31]Augereau, P., "Feedback Control of the Sound Inwardly Radiated by an Aircraft Panel Excited by a Turbulent Boundary Layer," Inst. of Sound and Vibration Research, TM-869, Univ. of Southampton, Southampton, England, U.K., Aug. 2001.

P. J. Morris
*Associate Editor*